ZURICH, SWITZERLAND
6 - 10 OCTOBER 2025

EUROPEAN GEOTHERMAL CONGRESS 2025

Modelling heat transport and thermosiphon flow in closed-loop deep geothermal systems

Vlasios Leontidis[1], Pietro Ungar[2], Paweł Wojnarowski[3], Thibaud Chevalier[1], Daniele Fiaschi[2], Leszek Pająk[3], Magnus Wangen[4], Christine Souque[1]

[1] IFP Energies nouvelles, 1 & 4 avenue de Bois Préau, 92852 Rueil-Malmaison, France

[2] Department of Industrial Engineering, University of Florence, Viale Morgagni 40, 50135, Firenze, Italy

[3] AGH University of Krakow, al. Adama Mickiewicza 30, 30-059 Kraków, Poland

[4] Institute for Energy Technology, Instituttveien 18, Kjeller 2027, Viken, Norway

vlasios.leontidis@ifpen.fr

Keywords: Closed-loop, CO2, thermosiphon.

ABSTRACT

Simulations are performed to demonstrate the use of CO_2 instead of water in deep geothermal coaxial borehole heat exchangers in three sites in France, Italy and Poland with different geological conditions. The reasons of circulating CO_2 are to enhance the heat recovery and to establish a natural recirculation due to the thermosiphon effect. For each site, a different well flow simulator is applied considering the detailed well configuration, the complete geological profile and the evolution of fluid's state and properties (pressure-temperature dependence). For comparison reasons simulations are performed with liquid water and CO_2. For the French site the low-temperature Paris basin is considered. Thermal energy production is limited in all tested cases, and water performs better. For the Italian case, a medium-high geothermal gradient area with a significant envisioned heating demand is selected. The CO_2-based configurations yield slightly lower outputs, delivering fluids with lower temperatures, but with higher natural pressurization when compared to H_2O. For the Polish conditions a common salt dome structure is chosen as a geothermal energy carrier. In the case of $scCO_2$, the surface system needs to be designed for high pressures, but some electricity production, besides heat, is possible. Thermal power of water-based case is higher, but electric power is negligible. In all three cases, the rapid decrease in the performance of the systems, either with water or CO_2, due to the cooling of the rocks around the wellbore is evident. For both fluids, self-circulation of the fluid, caused by the thermosyphon effect, is achieved, but with CO_2 being more significant.

1. INTRODUCTION

The HOCLOOP project ("A circular by design environmentally friendly geothermal energy solution based on a HOrizontal Closed LOOP") aims to verify a novel geothermal closed loop solution for the extraction of heat from deep or shallow formation rocks. The solution is based on new drilling technology and solves the challenges of conventional construction of geothermal wells. The project aims to develop the tools to enable the innovative geothermal solution and to demonstrate the technology in a full-scale test operation. The work covers the development and validation of models for the heat flow and investigates the possibility for improving the energy production by using alternative to water fluids in different potential EU pilot sites.

Indeed, and in order to address the concerns raised about the viability and longevity of the closed wells, due to the limited generation of thermal energy and the rapid decrease with time in the production temperature, alternatives to water fluids are investigated (Hu et al. 2020). The use of fluids such as supercritical-CO_2 ($scCO_2$) can be advantageous when compared to water as they can provide an increase in the production pressure due to the natural thermosyphon effect (Esmaeilpour et al. 2022). Due to the large difference in fluid's density, caused by the temperature change along the downward and the upward sections, the pressure of the fluid will increase. Depending on the inlet conditions, this increase in pressure may be sufficient to overcome the pressure losses caused in the surface installations and allow the fluid to auto-circulate without the need to expend additional energy to pump it into the well.

Here, three different sites are considered ranging from low temperature silico-clastic reservoirs in France to medium-to-high temperature metamorphic reservoirs in Italy and salt structures in Poland. The utilization of the extracted heat varies by location, reflecting the distinct socio-economic conditions surrounding each proposed installation: in France and Poland, the heat is used for district heating, whereas in Italy, it is applied to cogeneration, producing both electricity and heat for a series of greenhouses. For each site, a different flow simulator is used to model from one hand the heat transport from the hosting formation to the fluid due conduction and the circulation of the fluid in the well, on the other hand. These tools are GWellFM, BHEModel2.0 and GWT, respectively. All models integrate Equation-of-States (EoS) and thermodynamic properties calculators for water and CO_2, among others. The impact of using CO_2 instead of water in closed-coaxial wells extended by a horizontal section is studied. The fluid is injected into the annular space and returns in the surface by the central tube.

2. METHODOLOGY

2.1 Numerical Tools

Three in-house numerical simulators are used in the study: GWellFM from IFPEN, BHEModel2.0 from UNIFI and GTW from IFE. All tools:

- are 1D and axisymmetric
- are semi-transient geothermal simulators in cylinder coordinates solving the equation for transient heat conduction for cooling or heating of the rock, assuming, however, stationary advective (by the fluid) and convective heat transport in the wellbore
- solve the momentum, energy and mass balances
- calculate the heat losses due to conduction and forced convection, as well as pressure losses due to friction and gravity.

GWellFM (Geothermal Well Flow Model) considers the single-phase flows of liquids and gases, the hydrodynamics of the two-phase downward and upward flows, constitutive laws for mixtures, and the heat exchange between the well completion and the surrounding formation (Leontidis et al. 2023). The model is fully compositional and, to perform thermodynamic calculations, a thermodynamic engine has been integrated into the code (de Hemptinne et al. 2023). Calculations are performed in thermodynamic equilibrium and several Equation-of-States are available (Cubic-Plus-Association, Peng-Robinson, GERG-2008, Kestin and others). The energy balance is solved based on enthalpy (Pressure-Enthalpy tracking) for more precise calculations when comes to fluids like CO_2.

BHEModel2.0 is based on the numerical integration of 1D mass, momentum and energy balances along the well using a Runge-Kutta scheme (Ungar 2024). The heat transfer between the well and the surrounding rocks has been evaluated using a well-known correlation that has been extended to account for the possible presence of a convective fluid in a reservoir around the well. A time convolution approach has been implemented for extending the correlation to cases with variable extraction rates as originally proposed by Zhang et al. (2011). The fluid properties and derivatives are directly retrieved with REFPROP (Lemmon et al. 2018).

GTW (Geo-Thermal-Well) is a single-phase and semi-transient geothermal simulator in cylinder coordinates (Wangen 2025). It is the coupling of a 1D pipe-flow solver with an implicit and transient temperature solver for the well flow and the rock. These two models are serially coupled, with the temperature solution from the cell-centred FVM (finite-volume method) model providing the 1D pipe model with the surrounding heat flow. In return, a solution from the 1D pipe model provides the FVM model with fluid properties for the pipe cells in the mesh. Two or three global iterations are normally sufficient for convergence for the pressure and temperature solutions. The FVM temperature solver applies an implicit formulation of the energy balance to simulate the transient cooling of the rock. The pipe simulator solves the equations for stationary mass-, momentum and energy conservation of the fluid. The fluid properties such as heat capacity, enthalpy, viscosity etc are taken from tables of pressure and temperature.

2.2 Model Validation

GWellFM and GTW have been recently benchmarked against analytical solutions for the case of water circulation in a deep coaxial closed heat exchanger (Leontidis et al 2025). Here, the same case (Table 1) of a closed coaxial L-shaped well with CO_2 being injected in the annular space is run with the three codes and the temperature and pressure of the fluid at the outlet are compared in Figure 1.

Table 1: Data of validation case.

	Variable	Unit	Value
Wellbore	Depth, D	m	4500
	Hor. Length, L	m	2000
Inner tubing	Inner diam., ID	cm	9.715
	Thickness, h	cm	2.312
	Roughness, ε	mm	0.045
	Conductivity, k	W/m/K	0.01
Casing	Inner diam., ID	Cm	27.939
	Thickness, h	Cm	0.856
	Roughness, ε	mm	0.045
	Conductivity, k	W/m/K	45
Rocks	Conductivity, k	W/m/K	2.423
	Density, ρ	kg/m^3	2360
	Capacity, C_p	J/kg/K	930
Inlet conditions	Temperature, T_{in}	°C	10
	Pressure, P_{in}	bar	50
	Flow rate, m	kg/s	5
Boundary conditions	Surface temp., T_{surf}	°C	20
	Gradient, g_T	°C/m	0.04

All three models show similar behaviour, predicting very similar values for the outlet temperature and pressure. The discrepancy in the findings between the three codes are mainly coming from the difference in the energy balance, the solution of the transient problem and the fluid's properties calculator. GWellFM considers the enthalpy of the fluid, whereas GTW and BHEModel solves the energy balance based on the temperature with extra terms for the thermal expansibility and compressibility. On the other hand, both GWellFM and GTW numerically solve the unsteady and 2D heat transfer expressed by the radial Fourier heat conduction equation, whereas BHEModel considers an analytical solution based on a time function. Another source of discrepancy is that the different simulators use slightly different data for CO_2. A slight difference in density as a function of pressure and temperature leads to different fluid pressure. The same applies to the enthalpy, the heat capacity, the fluid compressibility, and the thermal expansibility. A slight difference in these properties as a function of pressure and temperature may lead to slightly different results.

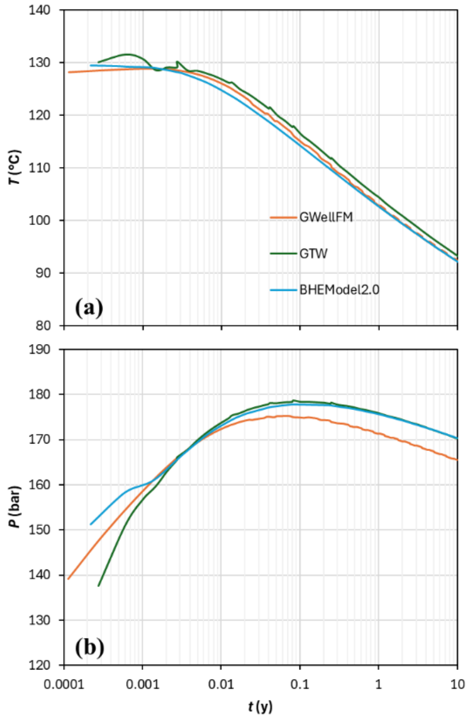

Figure 1: Model validation.

2.3 Study Cases

Three cases studies with different geological conditions are considered to test the HOCLOOP solution. The sites are located in France (FR), Italy (IT) and Poland (PL).

For the case of CO_2, it has been assumed to be maintained in a dense state (liquid or supercritical) throughout the loop), which requires the use of significantly higher pressures for the CO_2 when compared to water.

2.3.1 France, FR

The Parisian basin subsurface is exploited by deep geothermal doublets for district heating since 1969 and the density of the exploitation of the Dogger carbonates is the largest in the world with 50 doublets in activity. New reservoirs are targeted as the deeper and hotter Trias (up to 90 °C) or the shallower and more accessible lower cretaceous (35-40°C), both silico-clastic reservoirs. However, the Trias projects realised in the 1980's have failed due to a rapid loss of injectivity, and the lower Cretaceous recent realizations face similar difficulties. To reach the target of the French pluri-annual energy plan, different options must be considered, among which the HOCLOOP concept. The geological setting of this case study is representative of a sedimentary basin in thermal equilibrium and thus with a normal geothermal gradient. Tables A and B summarize the properties of the geological setting of the Paris basin and the geometry of the existing wellbore. Water and CO_2 as heat transfer fluids with different flow rates and different horizontal lengths are considered, according to Table 2.

Table 2: Case parameters (FR).

	Fluid	*L* (km)	*m* [kg/s]	T_{in} [°C]	P_{in} [bar]
Case 1	Water	2	3	25	6
Case 2	CO_2	1	3	20	100
Case 3	CO_2	2	3	30	100
Case 4	CO_2	2	10	20	100
Case 5	CO_2	2	3	20	120
Case 6	CO_2	2	3	30	100

In the case of the conventional geothermal doublets that are already in operation, the primary fluid is produced from a well at around 73°C with a 250 m^3/h (around 70 kg/s) flowrate, resulting in a total thermal energy of around 9-14 MW, depending on the reinjection temperature.

2.3.2 Italy, IT

Among the Italian three case studies analyzed in the scope of the HOCLOOP project, the most interesting one from a scientific perspective is the Gavorrano case. Gavorrano is a small village along the southern coast of Tuscany. It has originally attracted geologists' attention because of the presence of a pyrite mine and some abandoned quarries that allow a detailed reconstruction of the geological setting of the area (Brogi 2021). Even though it is located outside the traditional Larderello geothermal area, the geothermal gradient in the area is expected to be higher than 50°C/km (Vedova 2001), which makes it an appealing candidate for a closed loop application. The surrounding area has a significant heating demand due to the presence of multiple villages and small towns meaning that there could be an interest in developing a geothermal-powered district heating network (Fiaschi et al. 2025). Three well geometries have been analyzed in this case study (Table 3). The first two correspond to the economic optima for CO_2 and water, respectively, as identified by Fiaschi et al. (2025) using a simplified well model. Since the optimal geometries differ for CO_2 and water, a third case has been added to enable a direct comparison: CO_2 circulation in a well with the same geometry as the water-optimized configuration. Well diameters and inclinations are the same for all three cases and are described in Table C. The well description is simplified due to the fact that the presented analysis is just a preliminary evaluation. Inlet pressure and temperature were kept constant for both water (10°C, 6 bar) and CO_2 (10°C, saturated liquid conditions), while multiple flow rates were tested for each case. The range of CO_2 flow rates were higher than that of water, due to its lower specific heat capacity.

Table 3: Case parameters (IT).

	Fluid	Depth (km)	L (km)	*m* [kg/s]
Case 1	Water	4.25	3.75	5 - 15
Case 2	CO_2	3.25	2.375	10 - 25
Case 3	CO_2	4.25	3.375	10 - 30

2.3.3 Poland, PL

The case study in Poland evaluates salt structures, the Goleniów salt dome, as potential targets for applying the closed-loop technology developed in the HOCLOOP project. These structures are typically found in sedimentary basins where extensive salt deposits have formed and are one of the best geologically recognized forms. The northern Goleniów salt dome along the direction NNW-SSE has dimensions of 4.5 × 2.0 km. One exploration well has been drilled in the area. It reaches a depth of 3649 m and was drilled through the evaporite series of Zechstein from 888 m depth to 3649 m, reaching a thickness of >2761 m. Temperature profiling was performed in the depth interval up to 2800 m, where the temperature was measured at approximately 99°C. It should be added that the measurements were taken in unstable thermal conditions and in the lower part of the profile, you can see the temperature disturbance which required correction. The average geothermal gradient for Permian formations (salt dome) is at 2.5°C/100 m, while in the zone above the salt dome the geothermal gradient for Mesozoic formations is about 3.5°C/100 m. The average geothermal gradient for the entire profile in this area is about 3°C/100 m. Tables C and E summarize the properties of the geological setting, and the geometry of the wellbore assumed for analysis, while Table 4 shows the basic operating parameters of the HOCLOOP system adopted in each case.

Table 4: Case parameters (Poland).

	Fluid	*m* [kg/s]	T_{in} [°C]	P_{in} [bar]
Case 1	Water	5.556	35	6.1
Case 2	CO_2	10	35	140
Case 3	CO_2	15	35	140

4. RESULTS

4.1 France

Figure 2 and Figure 3 shows the evolution over time of fluid's temperature at the outlet of the return tube and the power production output (calculated throughout the study as the product of the mass flow rate and the enthalpy difference between outlet and inlet), respectively. In all cases, there is a rapid decrease of the temperature and the corresponding energy production due to the highly transient nature of the heat transfer mechanism. For water, this effect is more pronounced because water recovers more energy resulting in faster cooling of the surrounding rocks. However, water proved to be the optimal case, since the temperature of fluid is several degrees higher than that of CO_2.

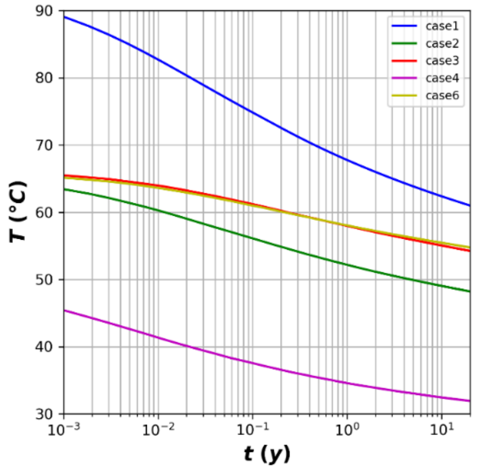

Figure 2: Evolution of outlet temperature (FR).

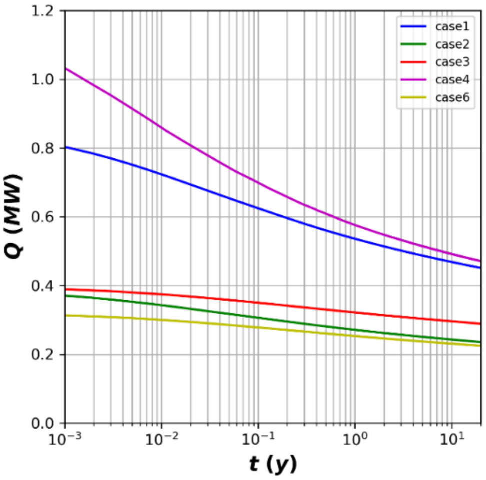

Figure 3: Evolution of gross thermal power production (FR).

CO_2 has higher energy only for the case of the higher flow rate, because the produced energy depends linearly on the flow rate. For the same case, the output temperature is the worst, because the fluid moves faster in the well resulting in lower residence time, thus, in lower heat recovery. In addition, the pressure losses due to the higher velocity are higher.

This can be seen in Figure 4 where the profiles of pressure and temperature along the well are traced. Except for Case 4, in all other cases with CO_2, the output pressure is higher than the injection pressure, which is caused by the thermosiphon effect and the impact of the decrease of fluid's density while travelling from the inlet to the outlet of the closed well. Only for the higher flow rate (Case 4), the outlet pressure is lower, because of the higher losses due to the friction. The pressure difference between outlet and inlet is higher for the lower flow rate, the lower injection temperature and the longer horizontal section.

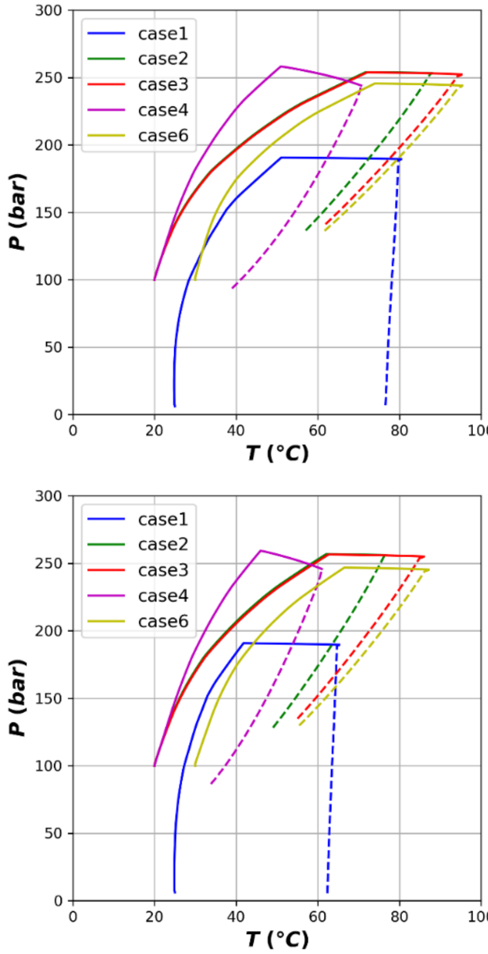

Figure 4: Pressure-Temperature profiles in the annular section (solid lines) and central tube (dashed lines) after 1 month (top) and 10 years (bottom) of operation (FR).

4.2 Italy

Due to the increased geothermal gradient and well length compared to the Paris case, the power extraction is expected to be much higher for the Italian case as can be seen in Figure 6. In particular, the water-based configuration (Case 1) is projected to extract more than 3 MW after 10 years of operation. The CO_2-based configurations yield slightly lower outputs: approximately 2.5 MW for the well with the same geometry as the water case (Case 3) and about 1.5 MW for the CO_2-optimized geometry (Case 2).

In terms of outlet temperature and pressure, the water-based system is expected to deliver a higher temperature fluid, but with limited natural pressurization. In fact, for flow rates exceeding 10 kg/s, pumping is required to maintain circulation. Conversely, CO_2 emerges from the well at a lower temperature but with significantly higher pressure, enabling natural circulation under a wider range of operating conditions.

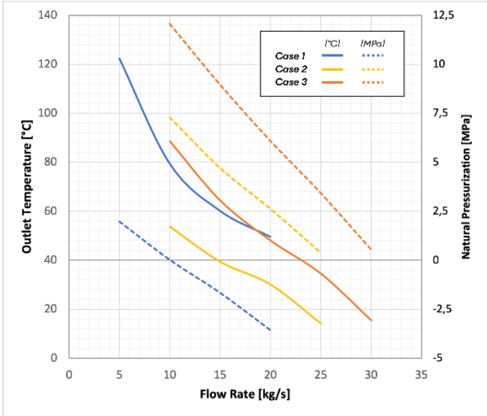

Figure 5: Outlet temperature and well pressure increase after 10 years (IT).

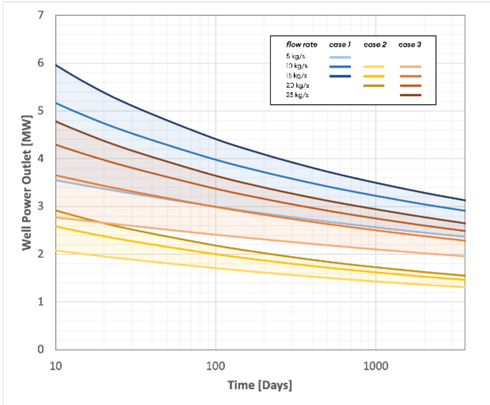

Figure 6: Predicted thermal power for the first 10 years of continuous operation (IT).

The lower energy output of the CO_2-based configuration is primarily due to reduced heat exchange with the surrounding rock per kilometre drilled, as shown in Figure 7. This occurs because the temperature difference between the rock and the fluid is smaller, a consequence of CO_2's temperature increasing with depth due to its high compressibility (Figure 8).

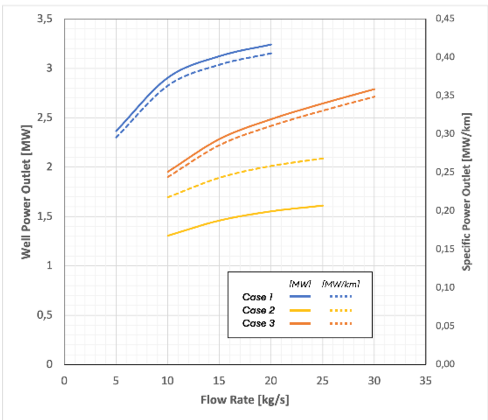

Figure 7: Predicted thermal power output after 10 years (IT). Solid lines: gross thermal power output; dashed lines: specific power output.

The real advantage of the CO_2-based system is that the energy is extracted in a more versatile form which can help increasing the profitability of the overall system despite the lower gross power output.

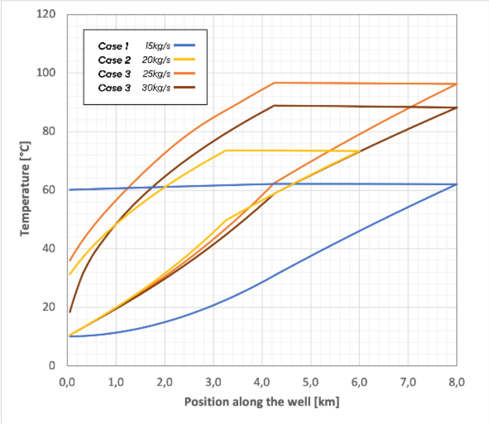

Figure 8: Temperature profile inside the well after 10 years of continuous operation (IT).

4.3 Poland

The next figures summarise the main results of the Polish case. Rapid stabilization of output parameters from the borehole heat exchanger is apparent in all cases with changes in the long term being small. It can be observed that increasing the CO_2 flow rate results in a decrease in temperature and output pressure. However, the total output power of the exchanger increases. In all cases, the thermosyphon effect is observed. Temperature changes with depth in the HOCLOOP exchanger are shown in Figures 12-13.
Table F shows a summary of the exchanger's input-output parameters after 20 years of operation.

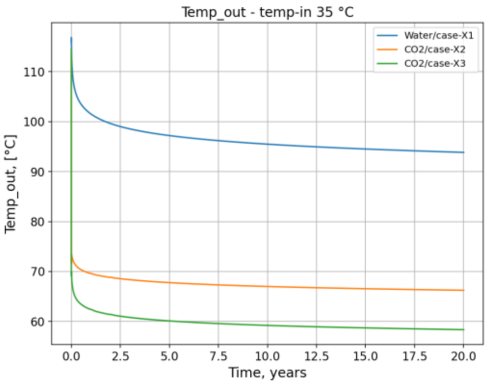

Figure 9: Changes in output temperature over time (PL).

In the case of carbon dioxide, the temperature in the deviated and vertical parts of the tubing significantly decreases compared to water, while in the horizontal section, it remains almost constant. This is due to changes in the properties of CO_2 as a function of temperature and pressure, as well as the Joule-Thomson effect. Throughout the system, CO_2 remains in a supercritical state.

Based on the data presented in
Table F, a more precise assessment of the possibilities of obtaining useful power is made. Since the obtained thermosyphon effect significantly exceeds the range of pressure losses in the surface installation, it is possible to think about using the energy of the working fluid related to the overpressure, in relation to the injection pressure, to generate electrical power.

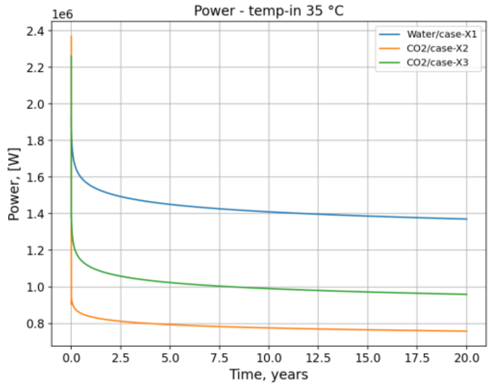

Figure 10: Output power over time (PL).

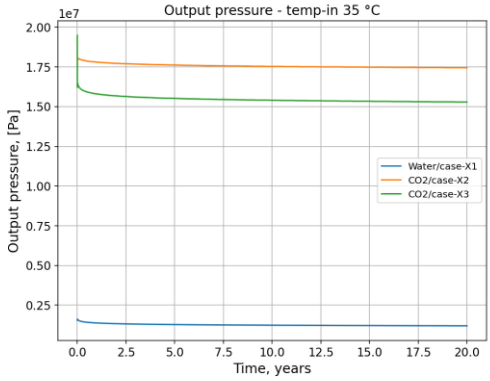

Figure 11: Output pressure over time (PL).

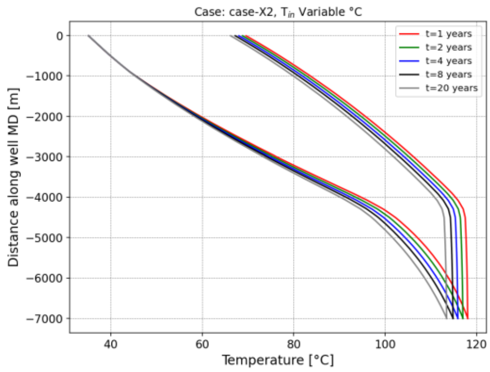

Figure 12: Temperature distribution (PL, case 2).

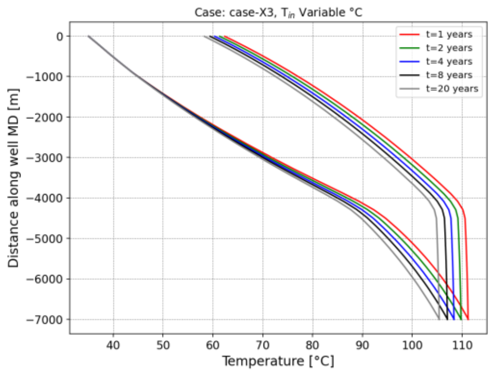

Figure 13: Temperature distribution (PL, case 3).

By assuming that the fluid flow resistance through the surface installation is 3 bar, then in addition to thermal power it is possible to generate electric power. Because the overpressure on the surface in the case of CO_2 is important, significant electric power can be expected. Electric power, W_{el} [W], in the case of water (case 1) is estimated as:

$$W_{el} = \frac{m(P_{out} - P_{in} - \Delta P)\eta_{wt}}{\rho} \quad \textbf{[1]}$$

where m is the flow rate [kg/s], P_{out} and P_{in} is output and inlet pressure [Pa], ΔP is the pressure losses in the surface energy system [Pa], ρ is the average density [kg/m^3] of water in the range of temperature and pressure between output and input and η_{wt} is the efficiency of water turbine (assumed as 0.75).

In the case of CO_2 is estimated based on the equation:

$$W_{el} = m(h_{out} - h) \quad \textbf{[2]}$$

where h_{out} is the enthalpy of CO_2 on output of the BHE [J/kg], h is the enthalpy of CO_2 after a supercritical CO_2 turbine [J/kg], estimated as:

$$h = h_{out} - \eta_{scCO_2}[h_{out} - h(P_{in} + \Delta P, T_{in})] \quad \textbf{[3]}$$

with η_{scCO2} the internal efficiency of supercritical CO_2 turbine (assumed as 0.9), $h(P_{in}+\Delta P,\ T_{in})$ the enthalpy [J/kg] of CO_2 in the pressure of the input to the borehole heat exchanger enlarged on pressure losses in the surface part of the installation (assumed to be equal 3 bar) and T_{in} the temperature at input to the borehole heat exchanger [K].

The thermal power of the system is estimated based on the equations:

- in the case of water:

$$P_{th} = mC_p(T_{out} - T_{in}) \quad \textbf{[4]}$$

- in the case of CO_2:

$$P_{th} = m[h'(P_{in} + \Delta P, T_{in}) - h_{in}] \quad \textbf{[5]}$$

where P_{th} is the thermal power of the solution [W], C_p is the mass specific heat capacity of liquid water, value average in the temperature and pressure range between T_{in}-T_{out} and P_{in}-P_{out} [J/(kg K)], $h'(P_{in}+\Delta P,\ T_{in})$ is the enthalpy of $scCO_2$ considering adiabatic expansion of the fluid from conditions at the deep borehole heat exchanger to pressure $P_{in}+\Delta P$ and temperature T_{in} [J/kg]. The value is higher on $h(P_{in}+\Delta P,\ T_{in})$ on internal $scCO_2$ turbine efficiency as follows:

$$\frac{h'(P_{in} + \Delta P, T_{in}) - h_{in}}{h'(P_{in} + \Delta P, T_{in}) - h_{in}} = \eta_{CO_2} \quad \textbf{[6]}$$

with h_{in} the enthalpy of CO_2 at input of the deep heat exchanger [J/kg],

Calculations are based on thermal properties of fluids estimated by CoolProp library ver. 6.1.1 (http://www.coolprop.org/index.html). Finally, based on the described assumptions, output powers are estimated and presented in
Table F.

3. CONCLUSIONS

The low-temperature French site seems not to be an optimal candidate for the closed-loop systems, especially when compared to the conventional geothermal applications. For all tested cases, the thermal output was relatively low, and water proved to be more performant when compared to $scCO_2$. The potential advantage of using CO_2 for creating a natural circulation due to the thermosiphon effect was shown through the increase in the outlet pressure.

The Italian case was much more promising given the higher geothermal gradient. Both water and CO_2 are expected to allow for the working fluid to naturally circulates in the well for lower flow rates with CO_2. Depending on the flow rate, outlet temperatures can be as high as 110°C but they will be significantly lower due to the need for a higher flow rate to obtain a substantial power outlet.

For the Polish site, the obtained results show that the variants assuming the use of CO_2 are characterised by lower thermal power, but higher electrical power. The obtained electrical power, in the case of considering the use of water, is very small, but the variants assuming the use of $scCO_2$ are more interesting in this aspect. The obtained electrical power can be used to drive other devices (e.g. pumps), providing a heat source as a self-sufficient system. Obtained thermal power looks promising because it can be used at the baseload of the power demand curve. It helps to repay financial expenditures.

The use of high injection pressures is required to maintain the CO_2 in its dense phase, and it is sure that brings technological challenges. On the other hand, may offer the possibility of electricity production, under certain geological conditions, and may lead to lower energy consumptions due to the induced self-circulation.

REFERENCES

Brogi, A., Caggianelli, A., Liotta, D., Zucchi, M., Spina, A., Capezzuoli, E., Casini, A., and Buracchi, E.: The Gavorrano Monzogranite (Northern Apennines): An Updated Review of Host Rock Protoliths, Thermal Metamorphism and Tectonic Setting, *Geosciences*, **11**, (2021).

Esmaeilpour, M., Gholami Korzani, M. and Kohl T.: Impact of thermosiphoning on long-term behavior of closed-loop deep geothermal systems for sustainable energy exploitation. *Renewable Energy*,**194** (2022).

Fiaschi, D., Ungar, P., Gigliotti, F., Meana-Fernandez, A., Thermo-Economic Analysis of a Geothermal-driven District Heating Network: comparison between a water-based and a CO2-based grid, Submitted to *Applied Thermal Engineering* (2025).

Hu, Z., Xu, T., Feng, B., Yuan, Y., Li, F., Feng, G. and Jiang, Z: Thermal and fluid processes in a closed-loop geothermal system using CO_2 as a working fluid, *Renewable Energy*,**154 (**2020).

Lemmon, E.W., Bell, I.H., Huber, M.L., and McLinden, M.O.: NIST Standard Reference Database 23: Reference Fluid Thermodynamic and Transport Properties-REFPROP, Version 10.0, National Institute of Standards and Technology, (2018).

Leontidis, V., Niknam, P.H., Durgut, I., Talluri, L., Manfrida, G., Fiaschi, D., Akin, S. and Gainville, M.: Modelling reinjection of two-phase non-condensable gases and water in geothermal wells, *Applied Thermal Engineering*, **223**, (2023).

Leontidis, V., Hernandez, E., Pogacnik, J., Wangen, M. and Harcouët-Menou, V.: Controlling injection conditions of a deep coaxial closed well heat exchanger to meet irregular heat demands: a field case study in Belgium (Mol), *Geothermal Energy*, **13**, (2025).

Ungar, P.: Use of CO2 as working fluid in geothermal systems, *PhD Thesis*, (2024)

Vedova, B.D., Bellani, S., Pellis, G., Squarci, P.: Deep temperatures and surface heat flow distribution, in: Vai, G.B., Martini, I.P. (eds) Anatomy of an Orogen: the Apennines and Adjacent Mediterranean Basins, 65-76,, *Springer*, Dordrecht (2001).

Wangen, M.: Numerical solutions for coaxial borehole heat exchangers using CO2 as a working fluid, *Applied Thermal Engineering*, **264**, (2025).

Zhang, Y., Pan, L., Pruess, K., & Finsterle, S.: A time-convolution approach for modeling heat exchange between a wellbore and surrounding formation. *Geothermics*, **40**, (2011)

Acknowledgements

The present research was funded by the European Union's Horizon Research and Innovation Program 10 under grant agreement No 101083558 (HOCLOOP Project).

Table A: Thermal properties of all geological layers for the Paris basin (France).

Layer	Bottom [m MD]	Temperature [°C]	Conductivity [W/m²/°C]	Capacity [J/°C/kg]	Density [kg/m³]
Surface	0	15	-	-	-
Albian	548	30.6	1.59	903	2380
Gault shale	608	32.6	3.16	859	2270
Barremian	754	38.3	1.63	915	2480
Oxfordian	1322	58.4	2.24	795	2390
Callovian	1623	68.1	1.73	917	2590
Lower Callovian	1727	71.7	2.14	805	2450
Bathonian	1767	73.7	2.14	806	2590
Dommerian	1963	81.0	1.74	915	2600
Rhetian	2146	88.0	2.63	887	2510
Anisian	2590	100.4	2.94	710	2370

Table B: Characteristics of the well completion in France.

Segment	Top [m MD]	Bottom [m MD]	Inclination [°]	Drilling [mm]	Casing ID [mm]
1	0	450	90	660.4	309.245
2	450	1100	50	431.8	198.755
3	1100	2090	49	304.8	198.755
4	2090	2276	49	215.9	198.755
5	2276	2590	49	215.9	198.755
6	2590	4590	0	194	175

Table C: Characteristics of the well completion in Italy (for section lengths see Table 3).

Segment	Inclination[°]	Drilling [mm]	Casing ID [mm]	Tubing OD [mm]	Tubing ID [mm]
1 (Vertical)	90	508	279.4	143	97
2 (Horizontal)	0	381	279.4	143	97

Table D: Estimated stratigraphic profile for salt dome case (Poland).

Depth [m]	Stratigraphy	Temperature [°C]
0	Quaternary	10
35	Tertiary	20
439	Cretaceous	40
657.6	Upper Jurassic	47
702.2	Permian	48
4300	Permian	126

Table E: The geometry of the wellbore assumed for analysis (Poland).

L [m MD]	ID [mm]	Inclination [°]
0 - 900	450.977	90
900 - 3690	313.6138	90
3690 - 4500	313.6138	34.931
4500 - 7000	216.789	0

Table F: Summary of the exchanger's input-output parameters after 20 years of operation (Poland).

					Output after 20 yeas		
	Fluid	Flow rate [kg/s]	T_{in} [°C]	p_{in} [MPa]	T_{out} [°C]	p_{out} [MPa]	Power divided into electricity and heat P_{el}/P_{th} [kW]
Case 1	Water	5.556	35	0.61	93.84	1.2	1 / 1 368
Case 2	CO_2	10	35	14	66.24	17.45	46 / 712
Case 3	CO_2	15	35	14	58.34	15.29	21 / 943